

RESEARCH LETTER

10.1002/2017GL076887

Key Points:

- The first lava flow thickness maps and new volume estimates are provided for the five eruptions at Hekla volcano in the 20th century
- The variable volume of the last three eruptions question if the production rate at Hekla volcano is very steady as previously proposed
- It is suggested that the excess pressure declines faster through the 20th century due to increased conduit resistance

Supporting Information:

- Supporting Information S1

Correspondence to:

G. B. M. Pedersen,
gro@hi.is

Citation:

Pedersen, G. B. M., Belart, J. M. C., Magnússon, E., Vilmundardóttir, O. K., Kizel, F., Sigurmundsson, F. S., et al. (2018). Hekla volcano, Iceland, in the 20th century: Lava volumes, production rates, and effusion rates. *Geophysical Research Letters*, 45. <https://doi.org/10.1002/2017GL076887>

Received 21 DEC 2017

Accepted 5 FEB 2018

Accepted article online 12 FEB 2018

©2018. The Authors.

This is an open access article under the terms of the Creative Commons Attribution-NonCommercial-NoDerivs License, which permits use and distribution in any medium, provided the original work is properly cited, the use is non-commercial and no modifications or adaptations are made.

Hekla Volcano, Iceland, in the 20th Century: Lava Volumes, Production Rates, and Effusion Rates

G. B. M. Pedersen^{1,2}, J. M. C. Belart^{1,3}, E. Magnússon¹, O. K. Vilmundardóttir⁴, F. Kizel⁵, F. S. Sigurmundsson^{3,4}, G. Gísladóttir⁴, and J. A. Benediktsson⁵

¹Institute of Earth Sciences, University of Iceland, Reykjavík, Iceland, ²Nordic Volcanological Center, University of Iceland, Reykjavík, Iceland, ³Laboratoire d'Etudes en Géophysique et Océanographie Spatiales, Centre National de la Recherche Scientifique (LEGOS-CNRS), Université de Toulouse, Toulouse, France, ⁴Institute of Life and Environmental Sciences, University of Iceland, Reykjavík, Iceland, ⁵Faculty of Electrical and Computer Engineering, University of Iceland, Reykjavík, Iceland

Abstract Lava flow thicknesses, volumes, and effusion rates provide essential information for understanding the behavior of eruptions and their associated deformation signals. Preeruption and posteruption elevation models were generated from historical stereo photographs to produce the lava flow thickness maps for the last five eruptions at Hekla volcano, Iceland. These results provide precise estimation of lava bulk volumes: $V_{1947-1948} = 0.742 \pm 0.138 \text{ km}^3$, $V_{1970} = 0.205 \pm 0.012 \text{ km}^3$, $V_{1980-1981} = 0.169 \pm 0.016 \text{ km}^3$, $V_{1991} = 0.241 \pm 0.019 \text{ km}^3$, and $V_{2000} = 0.095 \pm 0.005 \text{ km}^3$ and reveal variable production rate through the 20th century. These new volumes improve the linear correlation between erupted volume and coeruption tilt change, indicating that tilt may be used to determine eruption volume. During eruptions the active vents migrate 325–480 m downhill, suggesting rough excess pressures of 8–12 MPa and that the gradient of this excess pressure increases from 0.4 to 11 Pa s⁻¹ during the 20th century. We suggest that this is related to increased resistance along the eruptive conduit.

Plain Language Summary The sizes of volcanic eruptions are key parameters to understand eruption precursors and eruption hazard scenarios. Hekla is one of Iceland's most active volcanoes and erupted five times (1947–1948, 1970, 1980–1981, 1991, and 2000) during the 20th century. Here we use an archive of historical aerial photographs to reconstruct the topography before and after each eruption in order to provide the first precise lava thickness maps and volume estimates of Hekla volcano. Our results reveal that the last three eruptions ranged significantly in size unlike earlier estimates, indicating that the production rate at the volcano is more variable than previously thought. Furthermore, this suggests that geophysical measurements of the volcano deformation now correlate with the eruption size and therefore may be important to determine eruption size.

1. Introduction

Lava flow thicknesses, volumes, and effusion rates provide essential information for understanding the behavior of effusive eruptions and are important eruption parameters giving insight to eruption size and style. Furthermore, lava volumes are important in evaluating localized lava loading (Grappenthin et al., 2010; Murray, 1988; Ofeigsson et al., 2011), and lava volumes and thickness are critical for calibration of lava flow simulation models.

The volcano Hekla is one of the most active volcanic systems in Iceland and has erupted ~23 times since the settlement of Iceland in AD 874. These historical eruptions have primarily been studied by comparing literary sources with tephra chronological studies (Thórarinnsson, 1967), providing a volcanic record which suggests that the total erupted volume correlates linearly with the duration of the preceding repose period, indicating a constant production rate of 7 km³ dense rock equivalent (DRE) over the last 1,100 years (Thórarinnsson, 1967; Thórarinnsson & Sigvaldason, 1972). However, this estimate is based on tephra volumes assuming that the lava constitutes ~80% of the total eruption volume based on post-1,700 AD eruption volumes (e.g., Jakobsson, 1979; Thórarinnsson, 1967; Thordarson & Larsen, 2007).

Hekla mountain erupted 5 times (1947–1948, 1970, 1980–1981, 1991, and 2000) in the 20th century, producing tephra and basaltic-andesite lava flows. These five eruptions were monitored and have detailed descriptions of the course of events (e.g., Gronvold et al., 1983; Gudmundsson et al., 1992; Höskuldsson

Table 1
Eruption Parameters for the Five Eruptions at Hekla Mountain in the 20th Century

Lava flow field	Duration [d]	Repose time [yr]	th [m]	Area [km ²]	Lava [km ³]	MOR [m ³ s ⁻¹]	Lava DRE [km ³]	Tephra DRE [km ³]	Total DRE [km ³]	<i>E</i>	Production rate (10 ⁶ m ³ yr ⁻¹)
1947–1948	389	101	19	38.914	0.742 ± 0.086	22	0.631 ± 0.082	0.08 ± 0.04	0.711 ± 0.122	11.2	7
1970	61	23	12	17.128	0.211 ± 0.012	40	0.179 ± 0.012	0.03 ± 0.015	0.209 ± 0.027	14.7	9
1980	3	10	5	22.610	0.124 ± NA	479	0.105 ± NA	0.026 ± 0.013	0.131 ± NA	19.8	13
1981	7	1	11	4.365	0.047 ± NA	78	0.040 ± NA	NA	0.040 ± NA	0.0	40
1980–1981	10	10	7	24.549	0.170 ± 0.015	197	0.144 ± 0.014	0.026 ± 0.013	0.170 ± 0.027	15.3	17
1991	53	10	10	24.672	0.241 ± 0.019	53	0.205 ± 0.018	0.01 ± 0.005	0.215 ± 0.023	4.7	21
2000	12	9	7	14.587	0.095 ± 0.005	92	0.081 ± 0.004	0.004 ± 0.002	0.085 ± 0.006	4.7	9
20th century			11	122.276	1.452 ± 0.138	32	1.234 ± 0.131	0.150 ± 0.075	1.384 ± 0.206	10.8	

Note. Mean output rate (MOR) is based on the bulk lava volume and the eruption duration. The mean lava flow field thickness is denoted *th* and *E* is explosivity. DRE, dense rock equivalent.

et al., 2007; Thórarinnsson, 1967; Thórarinnsson & Sigvaldason, 1972). However, the lava volume estimates are uncertain because they are based on the planimetric method (Stevens et al., 1999), where the area of the flow field is multiplied by an estimated average lava thickness. Due to coarse sampling of lava thickness profiles, previous studies suggest that the planimetric volume estimates yields up to 50% uncertainties (Stevens et al., 1999; Wadge, 1978).

Here we address this problem by generating preeruption and posteruption digital elevation models (DEMs) for the last five eruptions from historical stereo photographs to produce the first lava flow thickness maps at Hekla volcano, Iceland. This enables high-precision estimates of lava volumes and effusion rates.

2. Data and Methods

Repeated aerial stereo-photogrammetric surveys have been conducted over Hekla since 1945. Seven sets of cloud-free aerial photographs from 1945 to 1992 were collected, covering the erupted lavas before and after each of the eruptions in 1947–1948, 1970, 1980–1981, and 1991. Additional orthorectified photographs from Loftmyndir ehf and DEMs from airborne Synthetic Aperture Radar (Guðmundsson et al., 2011; Magnússon, 2003), TanDEM-X (Rizzoli et al., 2016), and lidar were used in order to study the eruption in 2000. Furthermore, the lidar DEM, surveyed in 2015, was used as source of ground control points to constrain the photogrammetric campaigns. An overview of the quality of each data set is provided in Table S1 in the supporting information.

A series of DEMs and orthophotos from 1945 to 1992 were created using digital photogrammetric techniques (see Text S1 in the supporting information; Magnússon et al., 2016; Nuth & Käab, 2011). The difference of DEMs in a chronological sequence reveals the lava thickness from each eruption, and the orthophotos permit high-resolution mapping of the succession of lava flow fields. Hence, lava areas and volumes were calculated for each lava flow as well as for the entire flow field produced in each eruption (Tables 1 and S2). An accuracy assessment was performed in order to evaluate the uncertainty on the lava flow thicknesses by comparison of the derived elevation differences in areas where no changes were expected (Text S1). The lava volumes were converted to DRE, assuming $15 \pm 10\%$ vesicularity and the total volumes are calculated based on the DRE volume assuming a density of $2,550 \text{ kg m}^{-3}$ (Sigmondsson et al., 1992).

3. Eruptions at Hekla Volcano in 20th Century

3.1. Lava Thickness and Volumes

The thickness maps (Figure 1) cover each of the last five lava-producing eruptions and allow precise estimation of the lava flow volumes and the mean output rate, MOR (Harris et al., 2007). Along with the eruption parameters for the 1980–1981 eruption episode, details for the two individual eruptions in 1980 and 1981 are also provided. This is done by assuming that the average 1980 lava thickness outside the overlapping 1980 and 1981 lava field is representative for the entire 1980 lava field. Furthermore, our estimate of the 1981 eruption episode is a minimum estimate since our preeruption DEM does not take the erosion from the 1980 jökulhlaup into account (Gronvold et al., 1983).

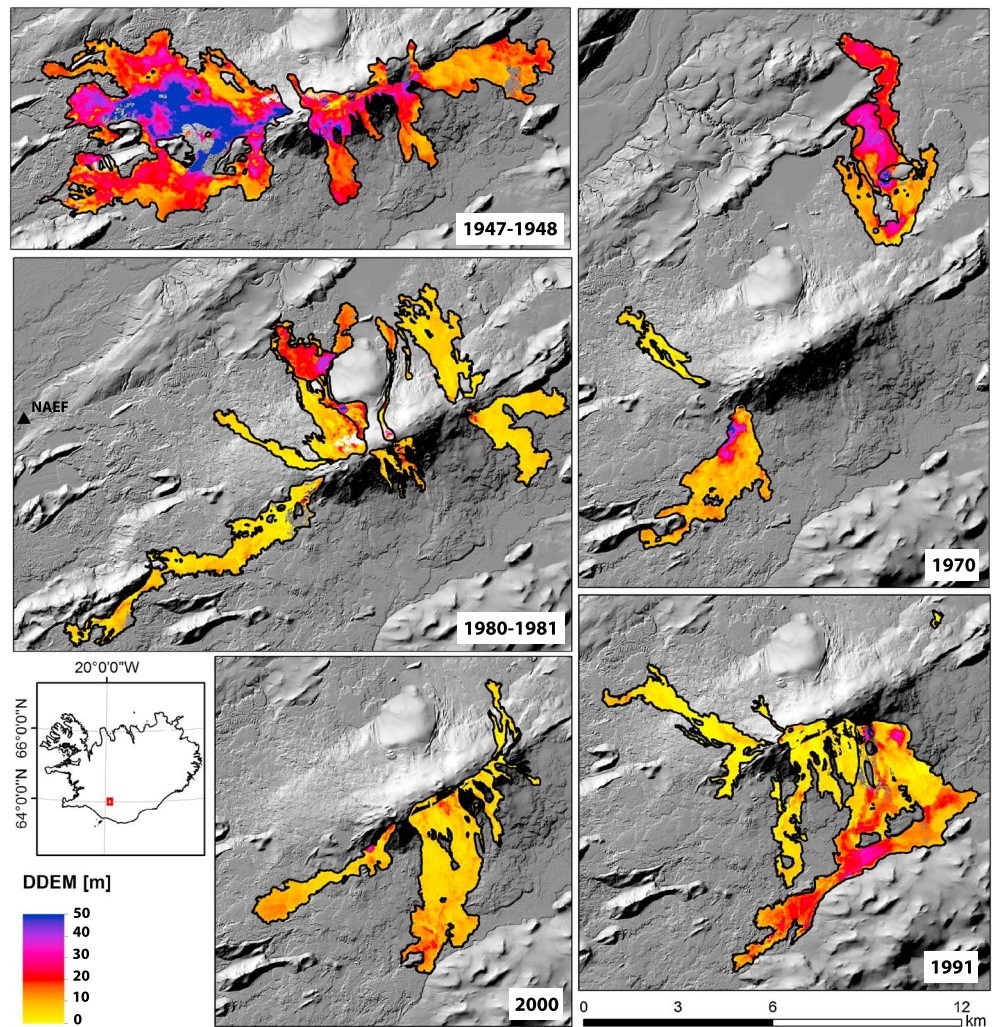


Figure 1. Lava flow thickness maps for Hekla Mountain in the 20th century. Background: hillshade from lidar digital elevation model (DEM), with gaps filled with TanDEM-X DEM. The Næfurholt tilt station, NAEF, is marked on the 1980–1981 map.

The average lava flow field thicknesses range from 5.5 m in the shortest eruption to 19.1 m in the longest eruption, while the bulk lava volume varies from $0.095 \pm 0.005 \text{ km}^3$ to $0.742 \pm 0.086 \text{ km}^3$ (Table 1). Combined with the previous published tephra volumes (assuming 50% uncertainty) from the last five eruptions (Thordarson & Larsen, 2007), the total erupted volume can be calculated. The lava volume is 80–100% of the total erupted volume, and hence, the explosivity (Thórarinnsson, 1967) varies from 0 to 20%.

The 1947–1948 eruption is the largest eruption and provides a bit more than half of the total erupted in the 20th century. The MOR values vary from 22 to $479 \text{ m}^3 \text{ s}^{-1}$, while the production rate varies from $7 \cdot 10^6$ to $40 \cdot 10^6 \text{ m}^3 \text{ yr}^{-1}$ during the century (Table 1 and Figure 2). The varying production rate is mainly caused by the varying volume of the last three eruptions (from $0.095 \pm 0.005 \text{ km}^3$ to $0.241 \pm 0.019 \text{ km}^3$), which each had a repose period of ~ 10 year (Figure 2a).

The eruption volume from 1845 to 2000 suggests an average production rate of $8.9 \cdot 10^6 \text{ m}^3 \text{ yr}^{-1}$, while the slope of the cumulative volume (Figure 2b) suggests $13 \cdot 10^6 \text{ m}^3 \text{ yr}^{-1}$ (from 1948 to 2000). Both estimates are significantly different from each other and are larger than previous estimates of $7 \cdot 10^6 \text{ m}^3 \text{ yr}^{-1}$ (Thórarinnsson, 1967).

3.2. Effusion Rates

The last five eruptions at Hekla followed the same pattern of high initial effusion rate, which quickly dropped and was followed by a period of slowly declining effusion rate reaching minimum of $\sim 1 \text{ m}^3 \text{ s}^{-1}$

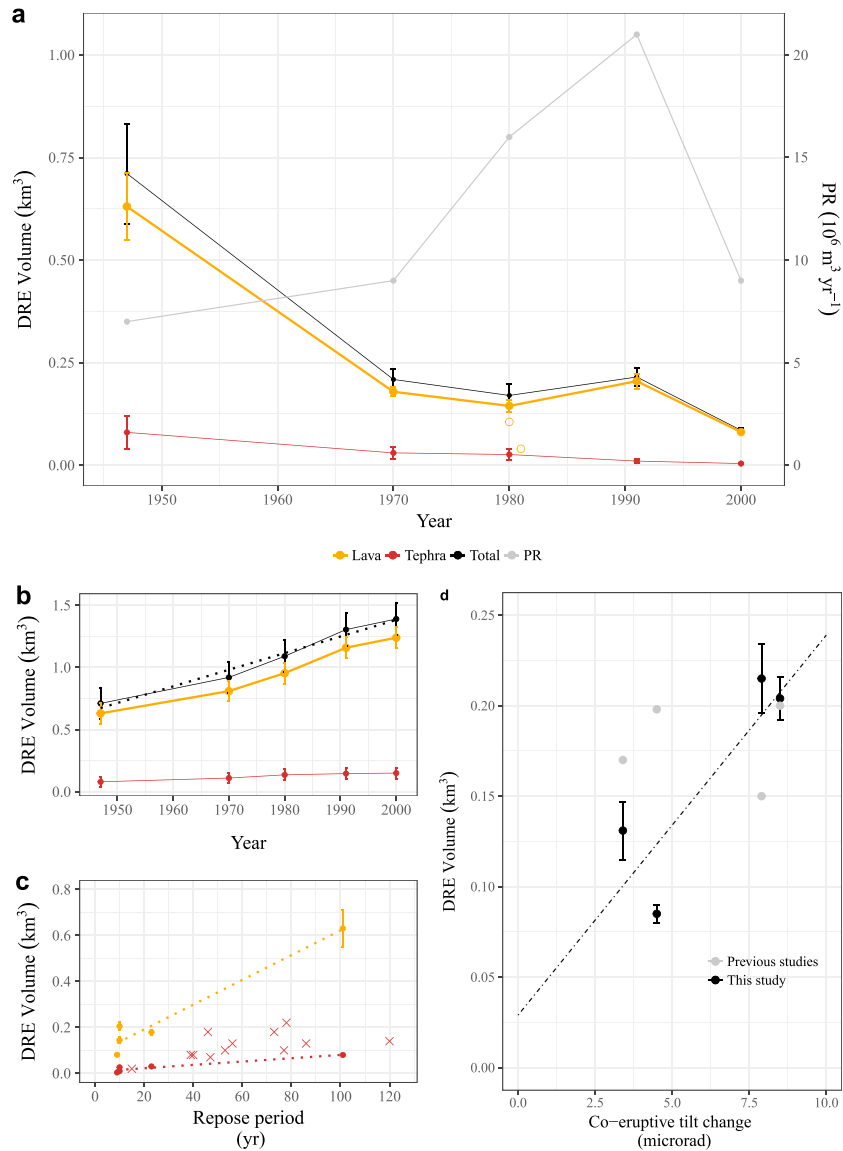


Figure 2. Erupted volumes at Hekla mountain in the 20th century. (a) Lava, tephra, and total eruption volumes and production rates, PR, (b) and cumulative volumes as a function of time. The hollow orange circles show the lava volumes from the 1980 and 1981 eruptions. (c) Erupted lava and tephra as a function of repose period. The crosses are estimated tephra volumes from historical, pre-20th century eruptions (Thordarson & Larsen, 2007). (d) Correlation between eruption volume and coeruptive tilt change at the station Næfurholt (Sturkell et al., 2013; Tryggvason, 1994). The regression lines are marked with dashed lines.

(Gudmundsson et al., 1992; Höskuldsson et al., 2007; Thórarinnsson, 1967, 1970). We therefore test if the effusion rate fit a simple exponentially declining (SED) effusion rate model for each eruption (see Text S2). These models are subsequently compared with observation of effusion rates (Figure 3).

In the 1947–1948 eruption, the effusion rate in the initial phase decreased in a near exponential fashion, and the eruption nearly ended after 5 days. After the central vents on the ridge shut down, the observed effusion rate went as low as 1–2 m³ s⁻¹ for 10 days, and then slowly, stepwise increased the next 50–60 days reaching a new maximum of nearly 100 m³ s⁻¹ 3.5 months into the eruption (Thórarinnsson, 1976). Likewise does the 1970 and 1991 eruption show delayed increase in effusion rate after 15 and 25–40 days, respectively (Gudmundsson et al., 1992; Thórarinnsson, 1970; Thórarinnsson & Sigvaldason, 1972), while there are no reports on increased effusion rates after the initial high effusion phase in the 2000 eruption.

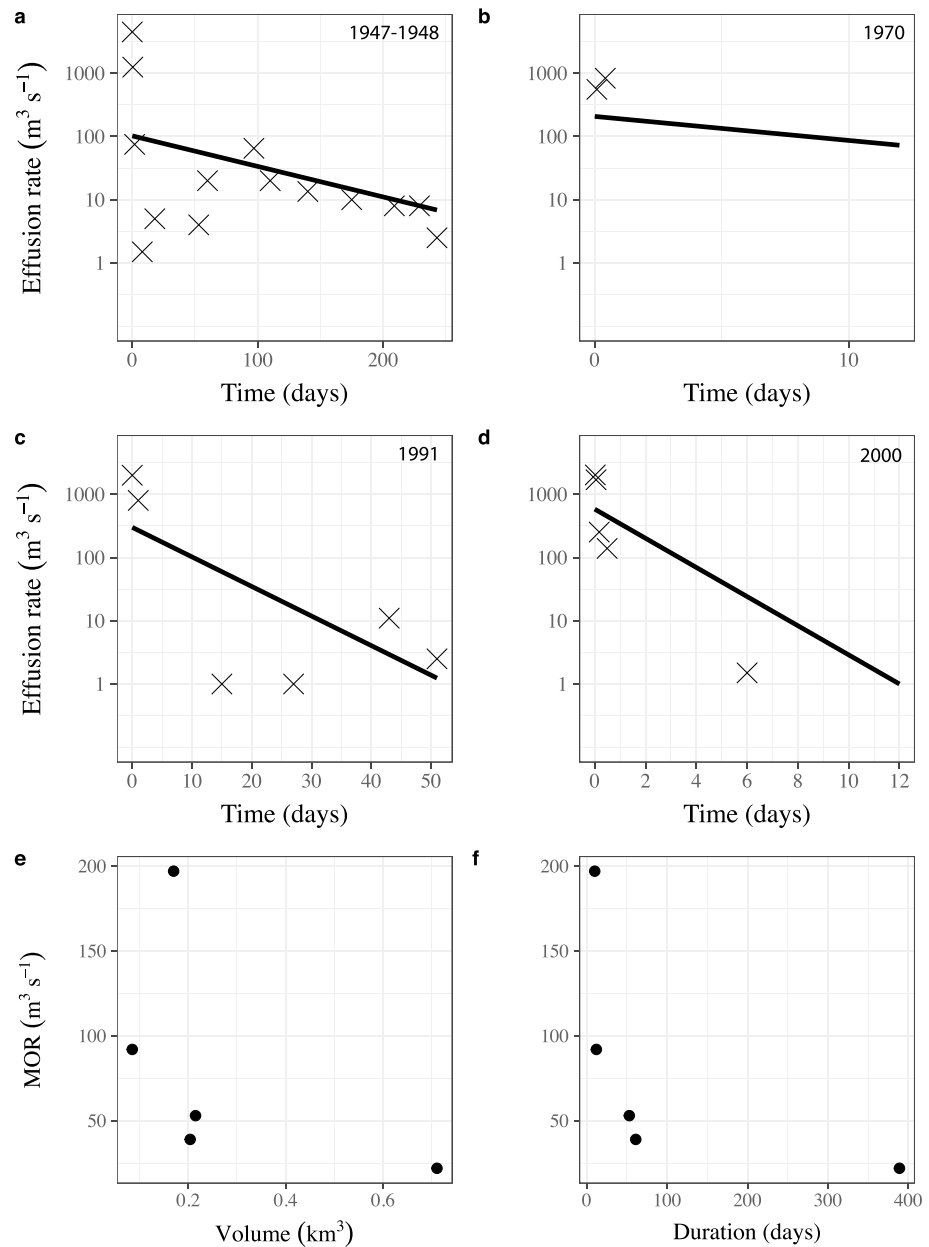


Figure 3. Simple exponentially declining models for the (a) 1947–1948, (b) 1970, (c) 1991, and (d) 2000 Hekla eruptions. Published effusion rate estimates are marked with black crosses (Gudmundsson et al., 1992; Höskuldsson et al., 2007; Thórarinnsson, 1976; Thórarinnsson & Sigvaldason, 1972). The y axis is in logarithmic scale. (e and f) Mean output rate values from the last five eruptions as a function eruption volume and duration.

The 1980–1981 eruption started with the initial 3 day eruption from 17–20 August 1980 which was followed by a 10 day eruption from 9 to 16 April 1981. There are no estimates of effusion rates from the 1980–1981 eruption, but our volume estimates reveal that the 1980 eruption has a MOR of $479 \text{ m}^3 \text{ s}^{-1}$, which is 5–20 times higher than any other eruption at Hekla in the 20th century. The tephra production during the renewed activity in 1981 was negligible (Gronvold et al., 1983); the eruption had MOR of $78 \text{ m}^3 \text{ s}^{-1}$ and the lavas were chemically indistinguishable from the 1980 eruption.

Overall, the SED models show poor correlation with the observed effusion rates. They underestimate the initial phase, overestimate the effusion rate after the initial phase, and do not fit the delayed increase in effusion rate as observed in 1947–1948, 1970, and 1991 eruptions.

4. Discussion

4.1. Lava Volumes and Production Rate in Hekla in the 20th Century

The high-resolution thickness maps of the last five Hekla eruptions improve the volume estimates for each eruption and for the 20th century as a whole. The previous estimates of the 1947–1948 (Thorarinsson, 1976) as well as the 1970 estimates (Thórarinnsson, 1970; Thórarinnsson & Sigvaldason, 1972) are within the uncertainty of our volume estimates of $0.742 \pm 0.086 \text{ km}^3$ and $0.205 \pm 0.012 \text{ km}^3$, respectively. The 0.150 km^3 volume estimates of 1980–1981 eruption (Gronvold et al., 1983) are slightly below our estimate of $0.169 \pm 0.016 \text{ km}^3$, probably due to an underestimation of the erupted lava volume in the 1981 eruption episode. There is a striking difference between the previous estimates on the 1991 and 2000 lava volumes and our estimates. The previously estimated 1991 lava volume (Gudmundsson et al., 1992) is ~60% of our estimate of $0.241 \pm 0.019 \text{ km}^3$, due to 3–4 m underestimation of average thickness. The estimate of the 2000 eruption (Höskuldsson et al., 2007) is ~200% of our estimate of $0.095 \pm 0.005 \text{ km}^3$, due to 3–4 m overestimation of the average thickness for the central and south vent flow. This reflects that the planimetric volume approach (Stevens et al., 1999) is associated with low accuracy because of the difficulty estimating the average thickness. The new eruption volume for the 2000 eruption fits the estimated volume decrease of $0.04\text{--}0.08 \text{ km}^3$ based on recorded coeruptive deflation (Ofeigsson et al., 2011). Moreover, it may explain some of the discrepancy between observed SO_2 release based on remote sensing (Rose et al., 2003) data and the calculated gas release (Moune et al., 2007).

The change in the 1991 and 2000 eruption volumes also improves the correlation between the measured E-W coeruptive tilt change at the Næfurholt station (Figure 1) and erupted volume (Sturkell et al., 2013; Tryggvason, 1994). The new data show approximately a linear relation between coeruptive tilt and the erupted volume, indicating that tilt measurements at this station can be used as a proxy to estimate the eruption volume (Figure 2d).

The production rate at Hekla mountain has varied from $7 \cdot 10^6$ to $40 \cdot 10^6 \text{ m}^3 \text{ yr}^{-1}$ during the 20th century and therefore question if Hekla has as a steady production rate as previously proposed (Gronvold et al., 1983; Hautmann et al., 2017; Kjartansson & Gronvold, 1983; Thórarinnsson & Sigvaldason, 1972). This proposition has been based on a suggested linear correlation between preceding repose time and eruption volume. Making the same plot with the new, precise lava volumes (on average ~90% total DRE volume) reveals a significant scatter for repose periods of ~10 years, and the slope of such a proposed correlation is badly constrained with only one data point for repose periods >20 years (Figure 2c). Since the proposition has been based on tephra volumes, we therefore also plot a linear regression line based on the tephra volumes from the 20th century against tephra volumes from 1,100–1,900 years (Thórarinnsson, 1967; Thordarson & Larsen, 2007). These data clearly plot above the regression line, and like the lava volumes, they reveal a significant scatter up to 0.1 km^3 DRE for eruption with similar repose periods (Figure 2c). Thus, the production rate at Hekla seems to be variable on 10–100 year time scale.

The total eruption volume from Hekla volcano in the 20th century is larger than any other Icelandic central volcanoes and is similar in size to the 6 month Holuhraun eruption in 2014–2015 (Pedersen et al., 2017). However, rates of higher productivity have been observed over shorter time periods, for example, during the Krafla fires (Harris et al., 2000). The productivity in Hekla seems to be comparable to Etna volcano and the outer rift zones of Piton de La Fournaise (Michon et al., 2015; Wadge et al., 1975) but is up to a magnitude smaller than Kilauea and Soufrière Hills (Poland, 2014; Wadge et al., 2010).

4.2. Effusion Rates in Hekla in the 20th Century

Hekla has been regarded as a closed volcanic system because of its preeruption and posteruption deformation pattern, the lack of venting, and the low degassing level (Ilyianskaya et al., 2015). The observed correlation between coeruptive deflation and eruption volumes supports that assumption. Furthermore, the observed MOR rates at Hekla are comparable in magnitude to episodic fissure eruptions from closed pressurized systems such as the 2014–2015 Holuhraun eruption, the 1975–1984 Krafla fires, the 2001–2012 Nyamulagira eruption, and the 1975–1976 and 2012–2013 Tolbachik eruptions (Albino et al., 2015; Dierschl & Rossi, 2018; Gudmundsson et al., 2016; Harris et al., 2000; Kubanek et al., 2017).

The SED models have been ascribed to apply to closed volcanic systems, where reservoir pressurization is released during eruptions by transfer of elastic strain energy stored in the reservoir rocks (Wadge, 1981).

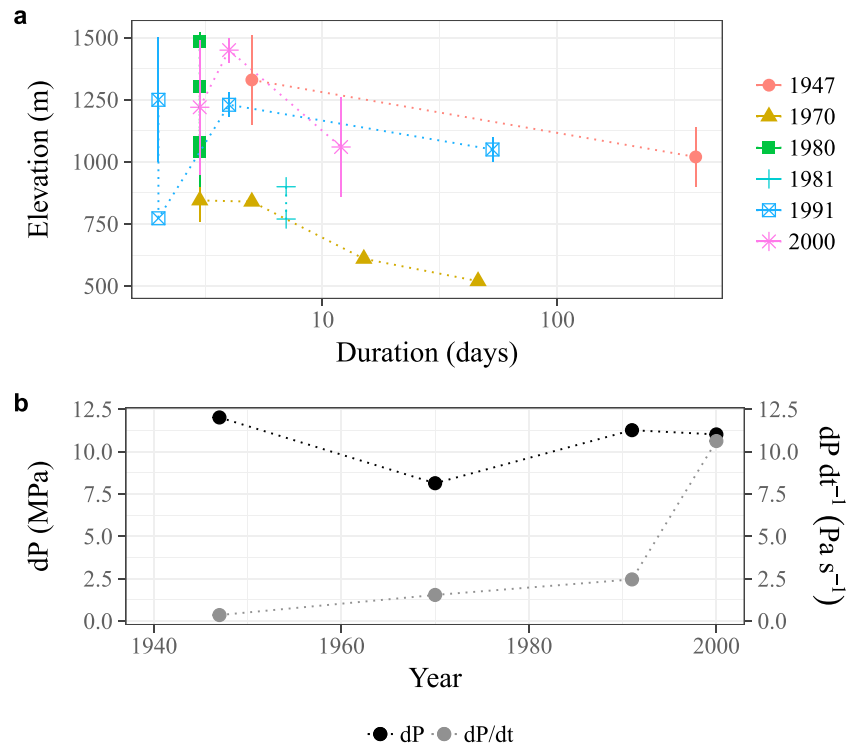


Figure 4. (a) Downhill vent migration during eruptions. Fissures that extend over an elevation range are marked with a vertical bar (see Table S2). (b) Pressure drop and pressure drop gradients for the 1947–1948, 1970, 1991, and 2000 eruption. There is no reported vent migration for the 1980–1981 eruption and therefore no estimates from this event.

The lava effusion is solely controlled by strain relaxation, and thus, large eruptions should be characterized by longer duration and higher MOR values.

Contradictory to what would be expected, the observed effusion rates during Hekla eruptions do not fit SED models and larger eruptions have lower MOR (Figure 3). This suggests that magma release and thereby lava effusion at Hekla is not solely controlled by release of strain energy and indicates that Hekla may not be a simple closed volcanic system.

The 1980–1981 eruption episodes and the 2000 eruption belong to a category of short, high MOR eruptions which suggest that processes (e.g., magmatic expansion) drain the reservoir faster than pure strain relaxation magma. On the other hand, the 1947–1948, 1970, and 1991 eruptions all lasted several weeks and have more moderate MOR values and a delayed increase in effusion rate. This category of eruptions does not fit the SED models either, and we suggest that conduit erosion over time scales of 2–4 weeks may have widened the conduit allowing sustained flow during lower magma pressures, producing the delayed increase in effusion rate. Another explanation can be that the pressure decrease caused by the initial erupted phase triggers deep-seated magma replenishment, which feeds the reservoir during longer eruptions and causes the delayed increase in effusion. This process could explain the late opening of the last vent in the 1970 eruption and the 1981 eruption episode. Our data cannot reveal if such magma replenishment could be due to buoyant flow tapping poroelastic crystal mush as suggested by Hautmann et al. (2017), but we suggest that a magma replenishment model should be able to explain increase of effusion rate from 1 to 100 m³ s⁻¹ within 2 months as observed in the 1947–1948 eruption.

The lava effusion at Hekla during the 20th century therefore reveals that multiple processes such as magmatic expansion, release of strain energy, conduit erosion, and magma replenishment all may impact the magma drainage, but at different time scales.

During the 1947–1948, 1970, 1991, and 2000 eruptions, the active vents migrate 325–480 m downhill (Figure 4), which is equivalent to a rough pressure drop during the eruption of 8–12 MPa (using same

parameters as Sigmundsson et al. (1992)). The pressure drop gradient is 0.4 Pa s^{-1} in the 1947–1948 eruption and increases through the 20th century to 11 Pa s^{-1} in 2000 (Figure 4d), indicating that the magma chamber loses the excess pressure faster. Sturkell et al. (2013) suggested that a sizable molten conduit evolved during the 1947–1948 eruption and that its dimensions have been sufficiently large to remain molten on the time scale of 10–20 years, equaling the repose periods after the 1947–1948 eruption. This molten conduit extends into the shallow crust, which has lower tensile strength compared to the rocks surrounding the magma reservoir, and thus, lower excess pressure is required before rupture, explaining the change of repose periods after the 1947–1948 eruption. This would also explain why the excess pressure required in the 1947–1948 eruption is around 12 MPa, significantly lower in the 1970 eruption (8 MPa) and then increases to ~ 11 MPa in the 1991 and 2000 eruption. Based on this model, the increase in the pressure drop gradient can be explained by increased hydrodynamic resistance along the conduit caused by cooling reducing the conduit radius. Each eruption would increase the conduit length and radius, but this increase would be smaller than the decrease due to cooling during repose periods, probably except for the case of the 1981 eruption. In the 2000 eruption the increased resistance caused the eruption to cease before the thermal erosion of the conduit system could allow more efficient magma evacuation as in the previous eruptions. This indicates that the conduit may be closing, and we may expect a change in eruptive frequency toward longer repose periods.

5. Conclusions

Lava thickness maps were produced for the five eruptions in the 20th century at Hekla volcano based on preeruption and posteruption elevation models generated from historical stereo photographs. These results provide precise estimation lava volumes: $V_{1947-1948} = 0.742 \pm 0.138 \text{ km}^3$, $V_{1970} = 0.205 \pm 0.012 \text{ km}^3$, $V_{1980-1981} = 0.169 \pm 0.016 \text{ km}^3$, $V_{1991} = 0.241 \pm 0.019 \text{ km}^3$, and $V_{2000} = 0.095 \pm 0.005 \text{ km}^3$. The production rate at Hekla mountain has varied from $7 \cdot 10^6$ to $40 \cdot 10^6 \text{ m}^3 \text{ yr}^{-1}$ during the 20th century and therefore question if Hekla has as a steady production rate as previously proposed. The new volumes suggest a linear correlation between coeruptive tilt change and erupted volume, indicating that the tilt station Næfurholt may be used to estimate the eruption volume.

A simple exponential declining effusion models cannot describe the effusion rate in Hekla eruptions during the 20th century and do not fit the initial high effusion phase nor the 15–25 days delayed increase in effusion observed in the 1947–1948, 1970, and 1991 eruptions. We therefore discard effusion rate model only controlled by elastic strain release and suggest that multiple processes such as magmatic expansion, release of strain energy, conduit erosion, and magma replenishment all may have impact the magma drainage in Hekla over different time scales.

During eruptions, the active vents migrate 325–480 m downhill, suggesting minimum pressure drop during eruption of 8–12 MPa. Through the 20th century the pressure drop gradient increased from 0.4 to 11 Pa s^{-1} in the 2000 eruption. We suggest this is related to increased resistance along the eruptive conduit and speculate that this increased resistance was responsible for ending the 2000 eruption before thermal erosion allowed the secondary effusion peak as observed in the other three eruptions.

Acknowledgments

The data used are listed in figure, tables, and supplements. The authors would first and foremost like to acknowledge the Icelandic Research Fund, Grant of Excellence 152266-052 (Project EMMIRS) for their financial support. Extended thanks go to two reviewers as well as Freysteinn Sigmundsson, Páll Einarsson, Michelle Parks, Stéphanie Dumont, and Benidikt Ófeigsson for useful comment. Carsten Kristinsson, the National Land Survey of Iceland, is thanked for providing the historical stereo photographs, and the German Space Agency is thanked for providing Tandem-X data through the Icelandic Volcanoes Supersite project supported by the Committee on Earth Observing Satellites.

References

- Albino, F., Smets, B., d'Oreye, N., & Kervyn, F. (2015). High-resolution TanDEM-X DEM: An accurate method to estimate lava flow volumes at Nyamulagira volcano (D. R. Congo). *Journal of Geophysical Research: Solid Earth*, *120*, 4189–4207. <https://doi.org/10.1002/2015JB011988>
- Dierschl, M., & Rossi, C. (2018). Geomorphometric analysis of the 2014–2015 Bárðarbunga volcanic eruption, Iceland. *Remote Sensing of Environment*, *204*, 244–259. <https://doi.org/10.1016/j.rse.2017.10.027>
- Grapenthin, R., Ófeigsson, B. G., Sigmundsson, F., Sturkell, E., & Hooper, A. (2010). Pressure sources versus surface loads: Analyzing volcano deformation signal composition with an application to Hekla volcano, Iceland. *Geophysical Research Letters*, *37*, L20310. <https://doi.org/10.1029/2010GL044590>
- Gronvold, K., Larsen, G., Einarsson, P., Thorarinnsson, S., & Saemundsson, K. (1983). The Hekla eruption 1980–1981. *Bulletin of Volcanology*, *46*(4), 349–363. <https://doi.org/10.1007/BF02597770>
- Gudmundsson, A., Oskarsson, N., Gronvold, K., Saemundsson, K., Sigurdsson, O., Stefansson, R., et al. (1992). The 1991 eruption of Hekla, Iceland. *Bulletin of Volcanology*, *54*(3), 238–246. <https://doi.org/10.1007/BF00278391>
- Gudmundsson, M. T., Jónsdóttir, K., Hooper, A., Holohan, E. P., Halldórsson, S. A., Ófeigsson, B. G., et al. (2016). Gradual caldera collapse at Bárðarbunga volcano, Iceland, regulated by lateral magma outflow. *Science*, *353*, aaf8988. <https://doi.org/10.1126/science.aaf8988>
- Guðmundsson, S., Björnsson, H., Magnússon, E., Berthier, E., Pálsson, F., Guðmundsson, M. T., et al. (2011). Response of Eyjafjallajökull, Torfajökull and Tindfjallajökull ice caps in Iceland to regional warming, deduced by remote sensing. *Polar Research*, *30*(1), 1–11. <https://doi.org/10.3402/polar.v30i0.7282>

- Harris, A. J. L., Dehn, J., & Calvari, S. (2007). Lava effusion rate definition and measurement: A review. *Bulletin of Volcanology*, 70(1), 1–22. <https://doi.org/10.1007/s00445-007-0120-y>
- Harris, A. J. L., Murray, J. B., Aries, S. E., Davies, M. A., Flynn, L. P., Wooster, M. J., et al. (2000). Effusion rate trends at Etna and Krafla and their implications for eruptive mechanisms. *Journal of Volcanology and Geothermal Research*, 102(3–4), 237–269. [https://doi.org/10.1016/S0377-0273\(00\)00190-6](https://doi.org/10.1016/S0377-0273(00)00190-6)
- Hautmann, S., Sacks, S. I., Linde, A. T., & Roberts, M. J. (2017). Magma buoyancy and volatile ascent driving autocyclic eruptivity at Hekla volcano (Iceland). *Geochemistry, Geophysics, Geosystems*, 18, 3517–3529. <https://doi.org/10.1002/2017GC007061>
- Höskuldsson, A., Óskarsson, N., Vogfjörð, K., Gronvold, K., Pedersen, R., & Ólafsdóttir, R. (2007). The millennium eruption of Hekla in February 2000. *Bulletin of Volcanology*, 70(2), 169–182. <https://doi.org/10.1007/s00445-007-0128-3>
- Ilyianskaya, E., Aiuppa, A., Bergsson, B., Napoli, R. D., Fridriksson, T., Óladóttir, A. A., et al. (2015). Degassing regime of Hekla volcano 2012–2013. *Geochimica et Cosmochimica Acta*, 159, 80–99. <https://doi.org/10.1016/j.gca.2015.01.013>
- Jakobsson, S. P. (1979). Petrology of recent basalts from the eastern volcanic zone, Iceland. *Acta Naturalia Islandica*, 26, 1–103.
- Kjartansson, E., & Gronvold, K. (1983). Location of a magma reservoir beneath Hekla volcano, Iceland. *Nature*, 301(5896), 139–141. <https://doi.org/10.1038/301139a0>
- Kubaneck, J., Westerhaus, M., & Heck, B. (2017). TANDEM-X time series analysis reveals lava flow volume and effusion rates of the 2012–2013 Tolbachik, Kamchatka fissure eruption. *Journal of Geophysical Research: Solid Earth*, 122, 7754–7774. <https://doi.org/10.1002/2017JB014309>
- Magnússon, E. (2003). Airborne SAR data from S-Iceland: Analyses, DEM improvements and glaciological application. MSc thesis, Department of Physics, University of Iceland.
- Magnússon, E., Muñoz-Cobo Belart, J., Pálsson, F., Ágústsson, H., & Crochet, P. (2016). Geodetic mass balance record with rigorous uncertainty estimates deduced from aerial photographs and lidar data—Case study from Drangajökull ice cap, NW Iceland. *The Cryosphere*, 10(1), 159–177. <https://doi.org/10.5194/tc-10-159-2016>
- Michon, L., Ferrazzini, V., Muro, A. D., Villeneuve, N., & Famin, V. (2015). Rift zones and magma plumbing system of Piton de la Fournaise volcano: How do they differ from Hawaii and Etna? *Journal of Volcanology and Geothermal Research*, 303, 112–129. <https://doi.org/10.1016/j.jvolgeores.2015.07.031>
- Moune, S., Sigmarsson, O., Thordarson, T., & Gauthier, P.-J. (2007). Recent volatile evolution in the magmatic system of Hekla volcano, Iceland. *Earth and Planetary Science Letters*, 255(3–4), 373–389. <https://doi.org/10.1016/j.epsl.2006.12.024>
- Murray, J. B. (1988). The influence of loading by lavas on the siting of volcanic eruption vents on Mt Etna. *Journal of Volcanology and Geothermal Research*, 35(1–2), 121–139. [https://doi.org/10.1016/0377-0273\(88\)90010-8](https://doi.org/10.1016/0377-0273(88)90010-8)
- Nuth, C., & Käab, A. (2011). Co-registration and bias corrections of satellite elevation data sets for quantifying glacier thickness change. *The Cryosphere*, 5(1), 271–290. <https://doi.org/10.5194/tc-5-271-2011>
- Ofeigsson, B. G., Hooper, A., Sigmundsson, F., Sturkell, E., & Grapenthin, R. (2011). Deep magma storage at Hekla volcano, Iceland, revealed by InSAR time series analysis. *Journal of Geophysical Research*, 116, B05401. <https://doi.org/10.1029/2010JB007576>
- Pedersen, G. B. M., Höskuldsson, A., Dürig, T., Thordarson, T., Jónsdóttir, I., Riishuus, M. S., et al. (2017). Lava field evolution and emplacement dynamics of the 2014–2015 basaltic fissure eruption at Holuhraun, Iceland. *Journal of Volcanology and Geothermal Research*, 340, 155–169. <https://doi.org/10.1016/j.jvolgeores.2017.02.027>
- Poland, M. P. (2014). Time-averaged discharge rate of subaerial lava at Kilauea volcano, Hawai'i, measured from TanDEM-X interferometry: Implications for magma supply and storage during 2011–2013. *Journal of Geophysical Research: Solid Earth*, 119, 5464–5481. <https://doi.org/10.1002/2014JB011132>
- Rizzoli, P., Martone, M., Gonzalez, C., Wecklich, C., Borla Tridon, D., Bräutigam, B., et al. (2016). Generation and performance assessment of the global TanDEM-X digital elevation model. *ISPRS Journal of Photogrammetry and Remote Sensing*, 132, 119–139. <https://doi.org/10.1016/j.isprsjprs.2017.08.008>
- Rose, W. I., Gu, Y., Watson, I. M., Yu, T., Blum, G. J. S., Prata, A. J., et al. (2003). The February–March 2000 eruption of Hekla, Iceland from a satellite perspective. In A. Robock & C. Oppenheimer (Eds.), *Volcanism and the Earth's atmosphere* (pp. 107–132). Washington, DC: American Geophysical Union. <https://doi.org/10.1029/139GM07>
- Sigmundsson, F., Einarsson, P., & Bilham, R. (1992). Magma chamber deflation recorded by the global positioning system: The Hekla 1991 eruption. *Geophysical Research Letters*, 19, 1483–1486. <https://doi.org/10.1029/92GL01636>
- Stevens, N. F., Wadge, G., & Murray, J. B. (1999). Lava flow volume and morphology from digitized contour maps: A case study from Mount Etna, Sicily. *Geomorphology*, 28(3–4), 251–261. [https://doi.org/10.1016/S0169-555X\(98\)00115-9](https://doi.org/10.1016/S0169-555X(98)00115-9)
- Sturkell, E., Ágústsson, K., Linde, A. T., Sacks, S. I., Einarsson, P., Sigmundsson, F., et al. (2013). New insights into volcanic activity from strain and other deformation data for the Hekla 2000 eruption. *Journal of Volcanology and Geothermal Research*, 256, 78–86. <https://doi.org/10.1016/j.jvolgeores.2013.02.001>
- Thórarinnsson, S. (1967). *The eruption of Hekla 1947–1948 I: The eruptions of Hekla in historical times. A tephrocronological study, Soc. Scientiarum Islandica* (pp. 1–171). Reykjavik.
- Thórarinnsson, S. (1970). *Hekla*. Reykjavik, Almenna Bokafélagid.
- Thórarinnsson, S. (1976). *The eruption of Hekla 1947–1948 IV: Course of events, Soc. Scientiarum Islandica* (pp. 1–44). Reykjavik.
- Thórarinnsson, S., & Sigvaldason, G. E. (1972). The Hekla eruption of 1970. *Bulletin of Volcanology*, 36(2), 269–288. <https://doi.org/10.1007/BF02596870>
- Thordarson, T., & Larsen, G. (2007). Volcanism in Iceland in historical time: Volcano types, eruption styles and eruptive history. *Journal of Geodynamics*, 43(1), 118–152. <https://doi.org/10.1016/j.jog.2006.09.005>
- Tryggvason, E. (1994). Observed ground deformation at Hekla, Iceland prior to and during the eruptions of 1970, 1980–1981 and 1991. *Journal of Volcanology and Geothermal Research*, 61(3–4), 281–291. [https://doi.org/10.1016/0377-0273\(94\)90009-4](https://doi.org/10.1016/0377-0273(94)90009-4)
- Wadge, G. (1978). Effusion rate and the shape of aa lava flow-fields on Mount Etna. *Geology*, 6(8), 503–506. [https://doi.org/10.1130/0091-7613\(1978\)6%3C503:ERATSO%3E2.0.CO;2](https://doi.org/10.1130/0091-7613(1978)6%3C503:ERATSO%3E2.0.CO;2)
- Wadge, G. (1981). The variation of magma discharge during basaltic eruptions. *Journal of Volcanology and Geothermal Research*, 11(2–4), 139–168. [https://doi.org/10.1016/0377-0273\(81\)90020-2](https://doi.org/10.1016/0377-0273(81)90020-2)
- Wadge, G., Herd, R., Ryan, G., Calder, E. S., & Komorowski, J.-C. (2010). Lava production at Soufrière Hills volcano, Montserrat: 1995–2009. *Geophysical Research Letters*, 37, L00E03. <https://doi.org/10.1029/2009GL014666>
- Wadge, G., Walker, G. P. L., & Guest, J. E. (1975). The output of the Etna volcano. *Nature*, 255(5507), 385–387. <https://doi.org/10.1038/255385a0>